

## Influence of substrate heterogeneities on the spreading of a drop

A. M. Cazabat,<sup>1</sup> J. De Coninck,<sup>2</sup> S. Hoorelbeke,<sup>2</sup> M. P. Valignat,<sup>1</sup> and S. Villette<sup>1</sup>

<sup>1</sup>Collège de France, Laboratoire de Physique de la Matière Condensée, Place Marcelin Berthelot, 11, 75231 Paris Cedex 05, France

<sup>2</sup>Université de Mons-Hainaut, Service de Physique Statistique et Probabilités, Place du Parc, 20, 7000 Mons, Belgium

(Received 24 November 1993)

The dynamics of spreading of monolayers of completely wetting liquids on substrates with various degrees of heterogeneity is studied here experimentally and numerically at a microscopic level. The radius of spreading of the first layer of the drop always presents two different diffusive regimes as a function of time if the temperature is higher than the two-dimensional (2D) critical temperature of the liquid. The associated spreading rate increases when the substrate becomes heterogeneous at the molecular scale. If the temperature is lower than the 2D critical temperature of the liquid, the second diffusive regime occurs only on heterogeneous substrates. The spreading rate again increases with the substrate heterogeneity, at least for weak heterogeneities. The agreement between the experimental results and the simulation, using the Kawasaki double spin exchange dynamics [K. Kawasaki, in *Phase Transitions and Critical Phenomena*, edited by C. Domb and M. S. Green (Academic, London, 1972), Vol. 2] is very satisfactory.

PACS number(s): 68.45.Gd, 02.70.Lq, 68.15.+e

### I. INTRODUCTION

Considerable interest has been devoted to the study of the spreading of a drop on top of a substrate. Different numerical approaches based on Monte Carlo and molecular-dynamics simulations have been performed to reach a better understanding of the experiments at a microscopic level [1–4]. In particular, different results have been obtained by Yang, Koplik, and Banavar [5,6] and Abraham *et al.* [7] using the same technique based on molecular dynamics, but for two different substrates: one modeled by five layers of molecules in [5,6], and the other by an idealized flat substrate in [7]. Both simulations recover the existence of a precursor film but they disagree on the time dependence of the growing of the film: a  $\sqrt{\log(t)}$  regime in the first case and a  $t$  behavior in the second case.

The technique we used in [1], based on Monte Carlo simulations, was in complete agreement with the experimental data. Two diffusive regimes for the radius of the first layer were observed: the first one corresponding to the spreading of the successive layers forming the drop, and the second one to the late disintegration of the monolayer. To reproduce this second diffusive regime in our simulations with homogeneous surfaces, we had to consider a special range of temperatures: below the critical point for the three-dimensional (3D) liquid (to keep constant the volume of the drop) but above the associated 2D critical point ( $T_c^{2D} < T < T_c^{3D}$ ). Indeed, whenever all the molecules are in contact with the wall, i.e., they belong to the first layer, the system becomes a 2D liquid. Above its critical temperature, we observe the formation of the gas phase which leads to the appearance of this second regime.

However, this simulation did not capture the whole experimental situation. The observation of a second diffusive process depends not only on the liquid-liquid in-

teractions, but also on the surface state. This is illustrated by the fact that monolayers of the same liquid will spread or not on different substrates which are completely wetted at the macroscopic scale.

Let us present the methodology we used to observe this property.

The thickness profiles of the drops are recorded by spatially resolved ellipsometry as a function of elapsed time. The experimental setup has been described elsewhere [2,3]. Figures 1 and 2 provide an example of the intriguing behavior mentioned above.

The liquid used is the same for all the experiments, i.e., polydimethylsiloxane (PDMS), molecular weight  $7.3 \text{ kg mol}^{-1}$ , polydispersity index 1.10, and surface tension  $21 \times 10^{-3} \text{ N m}^{-1}$ . The first substrate is bare silica, or more precisely, a silicon wafer covered with  $20 \text{ \AA}$  of natu-

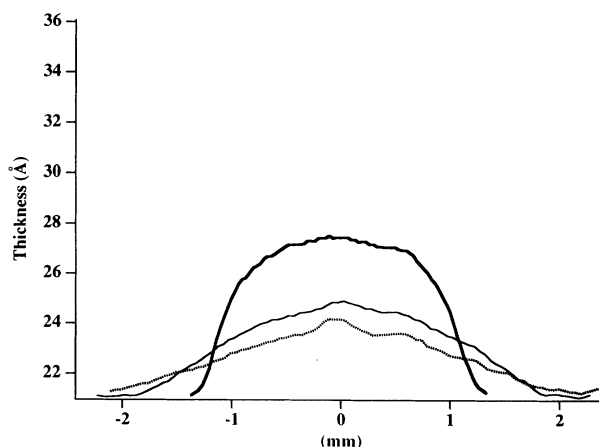


FIG. 1. Ellipsometric profiles of a monolayer of PDMS on a bare wafer. First profile (thick line) after 4 h, second (thin line) after 27 h, and third (dotted line) after 68 h.

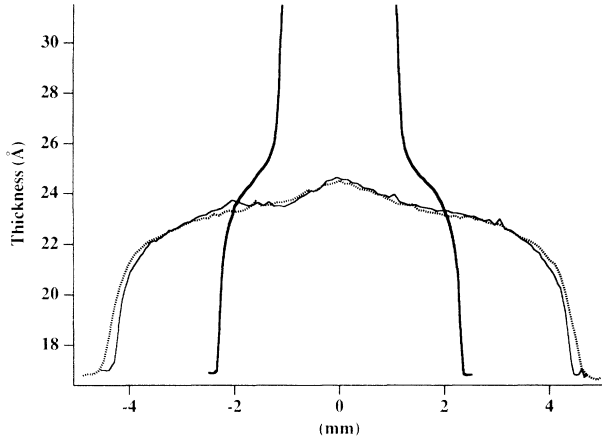


FIG. 2. Ellipsometric profiles of a monolayer of the same PDMS on a wafer bearing a grafted layer of trimethyl groups. Critical surface tension of the substrate,  $23 \times 10^{-3} \text{ N m}^{-1}$ . First profile (thick line) after 4 h, second (thin line) after 9 days, and third (dotted line) after 26 days.

ral oxide and cleaned using the uv-ozone procedure [8]. The second substrate is again an oxidized silicon wafer, but put in contact with the vapor of hexamethyldisilazane (HMDZ), thus bearing a grafted layer of trimethyl groups. The critical surface tension [9] of the silica for the series of linear alkanes is around  $27 \times 10^{-3} \text{ N m}^{-1}$ . The wafer bearing a layer of trimethyls has a critical surface tension  $23 \times 10^{-3} \text{ N m}^{-1}$ . Both substrates are wetted by the oil and the thickness profiles of multilayered droplets are rather similar. On the contrary, the monolayers behave in a very different way: spreading is observed on bare silica, while the layer stays compact on the grafted substrate. We interpret these features, in agreement with our microscopic simulations, as being due to the larger heterogeneity of the bare surface compared with the grafted one, this heterogeneity being either chemical (adsorption sites with variable adsorption energies), geometrical (roughness), or both.

The consequences of this model are exposed in the following. In Sec. II, we describe the model used in the simulations of which the results are discussed in Sec. III. Complementary experiments are performed with various degrees of surface heterogeneity and the results appear in Sec. IV. Finally, we present the conclusion of this work in Sec. V.

## II. MODEL

Let us now present the model. We perform a Monte Carlo simulation on a 3D lattice for a drop in the presence of an impenetrable wall. Each site of the lattice may be occupied by one molecule or empty. This model is equivalent to a 3D Ising model [10] in which the cohesion between the molecules is described by some fixed positive constant  $J$  (here, for simplicity, we consider a nearest-neighbor interaction); the attraction of the wall which we choose of the van der Waals type in this qualitative analysis is represented by  $u_i$ :

$$u_i = \begin{cases} -B(x,y) & \text{if } i = 1 \\ -\frac{A}{i^3} & \text{if } i \neq 1, \end{cases} \quad (1)$$

where  $B(x,y)$  is a local function of the point  $(x,y)$  on the substrate, which corresponds to the short-range attraction between the molecules of the liquid and the substrate and  $A$  is a positive constant.

Within this formalism, we consider a particular initial configuration corresponding to a parallelepiped of occupied sites and then let the system evolve according to a Monte Carlo dynamics which preserves the total number of  $[+]$  spin and  $[-]$  spins; the volume of the drop is indeed kept fixed during the experiment. This is the Kawasaki double spin exchange dynamics [11,12]. The system we consider is of 3000 occupied sites. At each step, the spins  $(\sigma_i, \sigma_j)$  may interchange positions according to the Kawasaki algorithm with a probability of transition defined by

$$P([\sigma_i, \sigma_j] \rightarrow [\sigma_j, \sigma_i]) = \frac{1}{1 + e^{\frac{H(\sigma_j, \sigma_i) - H(\sigma_i, \sigma_j)}{kT}}}, \quad (2)$$

with all the other spins of the system being kept fixed,  $H$  the Hamiltonian,  $k$  the Boltzmann constant, and  $T$  the temperature. In our numerical simulations, we have considered a lattice of  $20 \times 1000 \times 100$  sites and appropriate boundary conditions (periodic in the  $x$  direction and free everywhere else on top of the substrate) with one million MCS per occupied site.

## III. RESULTS OF THE SIMULATION

As already pointed out in the Introduction, when the temperature  $T$  is such that  $T_c^{2D} < T < T_c^{3D}$ , we observe two diffusive regimes. The results of simulations using Monte Carlo dynamics with a pure substrate ( $B$  is fixed) [1] were in qualitative agreement with the experimental data on a lighter oil ( $M_p = 2 \text{ kg mol}^{-1}$ ) which was slightly volatile in two dimensions. We now consider Monte Carlo simulations in the presence of a substrate with impurities and in the two ranges of temperature  $T < T_c^{2D}$  and  $T_c^{2D} < T < T_c^{3D}$ ; different models for  $B(x,y)$  will be considered.

We study the evolution of the successive layers as a function of the time, the length of a layer being the distance between the boundaries of the layer in the  $y$  direction. To define these boundaries, we proceed as follows. For each layer, we determine the density of particles in the  $y$  direction. The boundaries of the layer are then defined as the values of  $y$ , respectively, below and above which the density is less than half of its maximum value. In the case of monolayers, the presence of holes, due to the disintegration of the layer, implies that the radius is more difficult to define.

To study the effect of impurities on spreading, the simplest case we can consider is to fix  $B(x,y) = 0$  for a certain fraction of sites of the substrate. We fix in the substrate 10% of sites with  $B(x,y) = 0$  and we first impose  $T > T_c^{2D}$ . We observe two diffusive regimes in  $\sqrt{t}$ . How-

ever, there is a difference between this case and the case of the pure substrate, and that, for the second diffusive regime, the spreading coefficient is greater in the case of the substrate with impurities than in the case of the pure substrate. In fact, two phenomena occur: the 2D liquid evaporates and the molecules avoid the nonfavorable sites of the substrate (sites with  $B = 0$ ).

As a remark, let us mention that if the number of impurities with  $B = 0$  becomes too large, then the drop stops spreading. That is the reason why we limit ourselves to relatively small fractions of impurities.

Another interesting case is given by  $B(x, y)$  taken randomly between 10 and 15 for 10% of the sites of the substrates and  $B = 15$  for the other 90%, the coupling constant for the long-range interaction being equal to 5. For a gaslike monolayer ( $T_c^{2D} < T < T_c^{3D}$ ), we obtain results analogous to the previous case, except that the avoidance of the unfavorable sites with  $10 < B(x, y) < 15$  is slower than in the case  $B = 0$ .

The conclusion of the first part of this work is that the diffusive constant for the second regime observed for  $T_c^{2D} < T < T_c^{3D}$  increases by the presence of a small fraction of impurities.

The second step now is to investigate the range of temperature  $T < T_c^{2D}$ . We reproduce in Fig. 3 the evolution of the four first layers of a drop which spreads on a substrate with 10% of sites with  $10 < B(x, y) < 15$  randomly. In Fig. 4, we can see the associated evolution of the fraction of occupied unfavorable sites with  $10 < B(x, y) < 15$ .

We observe, in Figs. 3 and 4, a first regime in  $\sqrt{t}$ , then a second regime in  $\sqrt{t}$  during the decrease of the fraction of occupied sites with  $10 < B(x, y) < 15$ , and finally a flat behavior when we recover the 2D liquid structure. In this range of temperatures, our results indicate that the second diffusive regime finds its origin in the fact that the

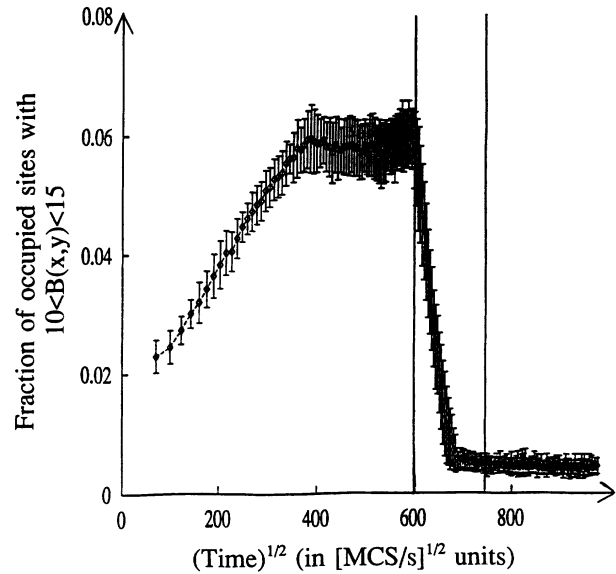


FIG. 4. Spreading of a drop with  $A = 5$ ,  $10 < B < 15$  for 10% of sites of the substrate ( $B = 15$  for 90% of sites),  $J = 0.05$ ,  $T = 0.1 < T_c^{2D} < T_c^{3D}$ : fraction of occupied sites with  $10 < B(x, y) < 15$  as a function of  $\sqrt{t}$  (in  $\sqrt{\text{MCS/s}}$  units).

molecules avoid the nonfavorable sites.

To study in more detail the second diffusive regime, we have performed Monte Carlo simulations for compact monolayers with 20% of impurities. By this way, the decrease of the fraction of occupied sites with  $10 < B(x, y) < 15$  takes place on a greater time scale since a molecule can only leave the "bad" site if there is a free site (without molecule) close to it. The results are reproduced in Figs. 5 and 6.

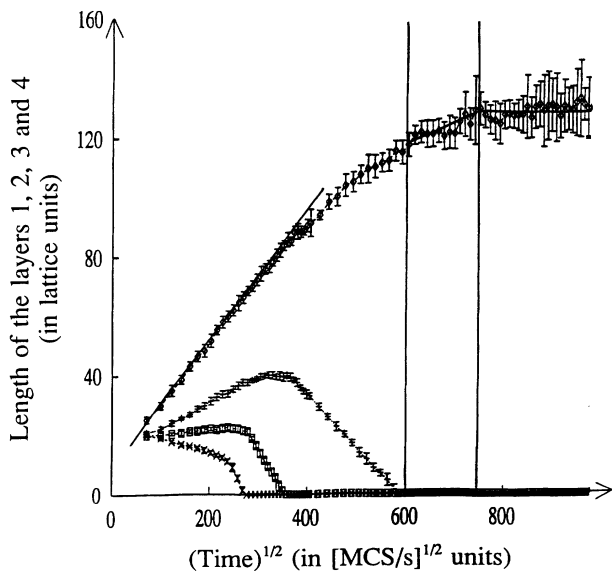


FIG. 3. Spreading of a drop with  $A = 5$ ,  $10 < B < 15$  for 10% of sites of the substrate ( $B = 15$  for 90% of sites),  $J = 0.05$ ,  $T = 0.1 < T_c^{2D} < T_c^{3D}$ : evolution of the radius of the four first layers (in lattice units) as a function of  $\sqrt{t}$  (in  $\sqrt{\text{MCS/s}}$  units).

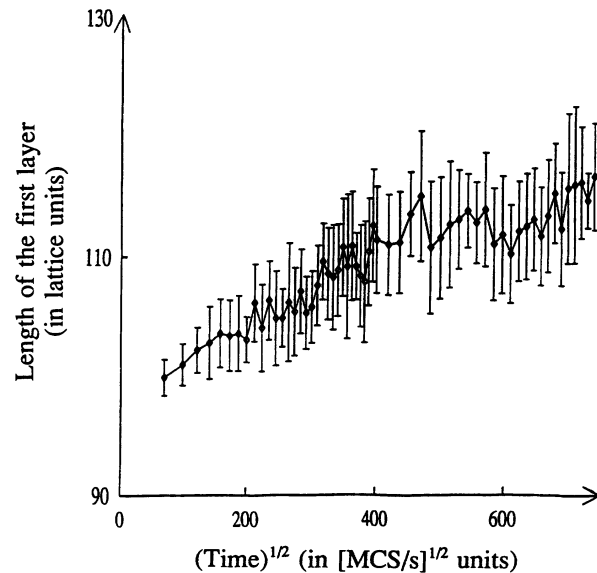


FIG. 5. Spreading of a compact monolayer with  $A = 5$ ,  $10 < B < 15$  for 20% of sites of the substrate ( $B = 15$  for 80% of sites),  $J = 0.05$ ,  $T = 0.1 < T_c^{2D} < T_c^{3D}$ : evolution of the radius of the first layer (in lattice units) as a function of  $\sqrt{t}$  (in  $\sqrt{\text{MCS/s}}$  units).

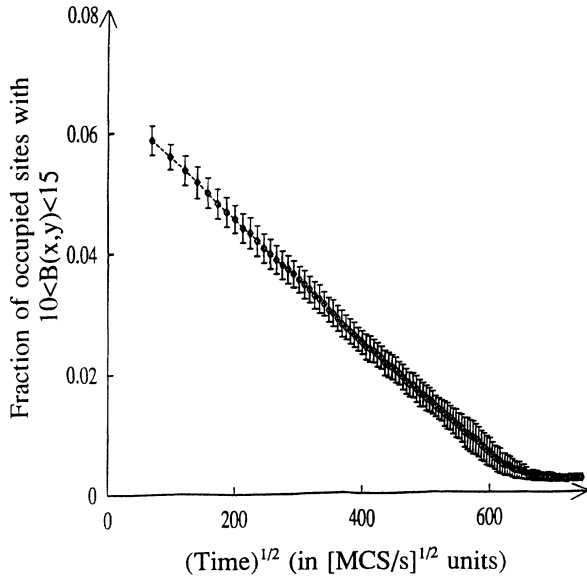


FIG. 6. Spreading of a compact monolayer with  $A=5$ ,  $10 < B < 15$  for 20% of sites of the substrate ( $B=15$  for 80% of sites),  $J=0.05$ ,  $T=0.1 < T_c^{2D} < T_c^{3D}$ : fraction of occupied sites with  $10 < B(x,y) < 15$  as a function of  $\sqrt{t}$  (in  $\sqrt{\text{MCS/s}}$  units).

In Fig. 5, we give the evolution of the length of the monolayer as a function of  $\sqrt{t}$  and, in Fig. 6, we give the evolution of the fraction of occupied sites with  $10 < B(x,y) < 15$ . We observe, in Fig. 5, a small growth of the monolayer between 100 and 120 in lattice units, during the decrease in Fig. 6. In fact, the molecules leave the sites characterized by  $10 < B(x,y) < 15$  which produces the growing of the monolayer. We do not reproduce the evolution of the monolayer after  $\sqrt{t} = 700$  (in units of  $\sqrt{\text{MCS/site}}$ ), because there appear to be too many holes in the layer to define its length. We have simulated the same monolayer, but with 10% of impurities. We observe a slower growth of the monolayer than in the case with 20% of impurities. In fact, the amplitude of the diffusion constant is intimately connected with the degree of impurities of the substrate at a low degree of impurities.

#### IV. EXPERIMENTAL STUDY

A systematic study of droplets of the same PDMS oil spreading on different surfaces has been performed. The following substrates have been used: (1) bare smooth wafers, cleaned with the uv-ozone procedure, and (2) smooth wafers bearing grafted layers of various compacity, obtained by slightly different grafting procedures.

##### A. Surface characterization

For each surface, the critical surface tension has been measured using the homologous series of linear alkanes. This gives a qualitative characterization of the trimethyl layer compacity [13]. Another piece of information on the surface heterogeneity is the contact angle hysteresis

TABLE I. Diffusion coefficients measured for the spreading of the monolayer on various substrates. The monolayer radius is measured at the bottom of the layer. The molecular weight of the oil is  $7.3 \text{ kg mol}^{-1}$ . Bare silica has been cleaned with the uv-ozone procedure. The grafted wafers have been put in contact with HMDZ for different times ( $\frac{1}{4}$  h and  $\frac{1}{2}$  h, respectively). No significant change in  $D$  and  $\theta_a - \theta_r$  is observed for longer contact times although the critical surface tension is reduced to  $22 \times 10^{-3} \text{ N m}^{-1}$ .

Substrate	$\gamma_c$ ( $10^{-3} \text{ N m}^{-1}$ )	$\theta_a - \theta_r$ (degrees)	$D$ ( $\text{m}^2 \text{ s}^{-1}$ )
Bare silica	$\approx 27$	$\approx 20$	$\approx 4 \times 10^{-12}$
HMDZ- $\frac{1}{4}$ h	$\approx 25$	$\approx 7$	$\approx 3.5 \times 10^{-13}$
HMDZ- $\frac{1}{2}$ h	$\approx 23$	$\approx 7$	$\approx 0.5 \times 10^{-13}$

of hexadecane on the substrate. The results are reported in Table I.

As expected, bare silica is the most heterogeneous smooth substrate. The presence of the grafted layer reduces the heterogeneity, and the substrate with the best homogeneity is the one with the compact grafted layer. Longer grafting times did not change significantly the behavior of the monolayer.

##### B. Experimental profiles

We performed a systematic study of the spreading of the same oil (molecular weight  $7.3 \text{ kg mol}^{-1}$ ) on the various substrates. The monolayers do not spread significantly on grafted surfaces, and the edges are quite steep as we can see in Figs. 2 and 7.

This tendency is more and more marked when the compacity of the grafting increases. This suggests that the oil is below its 2D critical temperature. On perfectly homogeneous surfaces, we would expect the layer not to spread at all.

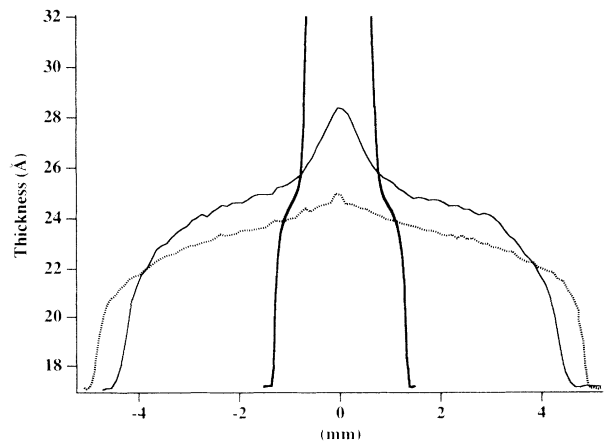


FIG. 7. Ellipsometric profiles of a monolayer of the same PDMS oil on a wafer bearing a grafted layer of trimethyl groups. Critical surface tension of the substrate,  $25 \times 10^{-3} \text{ N m}^{-1}$ . First profile (thick line) after 4 h, second (thin line) after 6 days, and third (dotted line) after 14 days.

On bare surfaces, significant spreading is observed like in Fig. 1. The width of the profiles increases, not because of the diffusion of a 2D gas phase, but because the layer breaks into islands or becomes dendritic, as also observed in Fig. 3. The third regime present in Fig. 3 is not reached with bare surfaces where the distribution of heterogeneities is wide. On grafted surfaces, the monolayer radius stops growing after typically one to two months. However, the noise on the records increases and no precise analysis of the profile can be done after this time.

Rough estimates of the diffusion coefficients associated with the growth of the monolayer radius with time are also given in Table I. These values are not really significant at long times for flattened layers, because a "radius" can be defined unambiguously only for well-defined profile shapes. Anyway, the trends are very clear: an increase in the grafted layer compacity is associated with a decrease in the diffusion coefficient.

Attempts to use rough surfaces obtained by chemical attack with hydrofluoric acid were not very convincing: the spreading of multilayered droplets is considerably accelerated, however this is no longer true for the monolayer. There is a considerable scattering of the values for the diffusion coefficients of the monolayer, but they are not larger than the ones on bare silica. Moreover, rough grafted surfaces behave as smooth grafted ones, i.e., the diffusion coefficients have very low values. Surface roughness possibly plays a role in the spreading of the monolayer, but we were not able to provide evidence of

this in the present study, where chemical heterogeneity is obviously the leading parameter.

## V. CONCLUSION

We have performed several simulations for the spreading of a drop on different substrates and at different temperatures. In the case of the pure substrate, we only observe two diffusive regimes when  $T_c^{2D} < T$ . In the case of the substrate with impurities, a second diffusive regime appears even if  $T < T_c^{2D}$ : the molecules avoid the non-favorable sites of the substrate and the amplitude of the diffusion coefficient is intimately connected with the fraction of impurities. In this line, experiments have been performed with various degrees of surface heterogeneity. We indeed observe that a monolayer spreads on a substrate with a higher heterogeneity whereas it does not spread on homogeneous surfaces (the oil being below its 2D critical temperature).

## ACKNOWLEDGMENTS

The authors acknowledge financial support from the Tournesol program and from the EEC, Contract No. JOUF-0020F(CD), which makes this collaboration possible. This text presents also research results of the Belgian program on Interuniversity Poles of Attraction initiated by the Belgian State, Prime Minister's Office, Science Policy Programming. We also thank G. Chavepeyer for useful chemical preparation of our substrates.

- 
- [1] J. De Coninck, N. Fraysse, M. P. Valignat, and A. M. Cazabat, *Langmuir* **9**, 1906 (1993).
  - [2] F. Heslot, N. Fraysse, and A. M. Cazabat, *Nature* **338**, 640 (1989).
  - [3] F. Heslot, A. M. Cazabat, P. Levinson, and N. Fraysse, *Phys. Rev. Lett.* **65**, 599 (1990).
  - [4] F. Heslot, A. M. Cazabat, and P. Levinson, *Phys. Rev. Lett.* **62**, 1286 (1989).
  - [5] J. Yang, J. Koplik, and J. R. Banavar, *Phys. Rev. Lett.* **67**, 3539 (1991).
  - [6] J. Yang, J. Koplik, and J. R. Banavar, *Phys. Rev. A* **46**, 7738 (1992).
  - [7] J. A. Nieminen, D. B. Abraham, M. Karttunen, and K. Kaski, *Phys. Rev. Lett.* **69**, 124 (1992).
  - [8] J. R. Vig, *J. Vac. Sci. Technol. A* **3**, 1027 (1985).
  - [9] W. Zisman, in *Contact Angle, Wettability and Adhesion*, edited by R. F. Gould, *Advances in Chemistry Series Vol. 43* (American Chemical Society, Washington, DC, 1964), p. 381.
  - [10] R. Pandit, M. Schick, and M. Wortis, *Phys. Rev. B* **26**, 5112 (1982).
  - [11] K. Kawasaki, in *Phase Transitions and Critical Phenomena*, edited by C. Domb and M. S. Green (Academic, London, 1972).
  - [12] *Monte Carlo Methods in Statistical Mechanics: An Introduction*, edited by K. Binder (Springer, Berlin, 1988).
  - [13] F. Tiberg and A. M. Cazabat, *Europhys. Lett.* **25**, 205 (1994).